P1.12

MESOSCALE VARIATIONAL ASSIMILATION OF PROFILING RADIOMETER DATA

Thomas Nehrkorn* and Christopher Grassotti

Atmospheric and Environmental Research, Inc.
Lexington, Massachusetts

Randolph Ware

Radiometrics Corporation
Boulder, Colorado

1. INTRODUCTION

The variational assimilation of measurements from a vertically pointing, ground-based 12-channel microwave profiling radiometer is tested with the MM5 3dvar and 4dvar data assimilation systems.

The Radiometrics TP/WVP-3000 radiometer measures brightness temperature in 7 microwave frequencies from 51 to 59 GHz on the flank of the 60 GHz oxygen resonance line and 5 frequencies from 22 to 30 GHz associated with the water vapor resonance peak at 22.2 GHz (see Ware et al. 2003, and references contained therein).

Retrieved profiles of temperature, water vapor, and cloud liquid water are obtained through neural net inversions of the brightness temperatures, where the neural net is trained using radiosonde soundings and corresponding forward modeled brightness temperatures. An observation operator has also been developed for the direct assimilation of the measured brightness temperatures, using the forward model and its adjoint.

The impact of assimilation of the retrieved profiles, and direct assimilation of the brightness temperatures, on analyses and subsequent forecasts have been tested using the MM5 mesoscale model and its associated 4dvar assimilation system. Results are presented here from two separate case studies: one using data from a profiler located at the ARM CART site in Oklahoma, another from a profiler on the NCAR Foothills campus in Boulder, Colorado.

The results demonstrate the proper implementation of the 4dvar assimilation of both retrieved profiles and brightness temperature data from the profiler. Forecast impacts are generally small in the cases studied here, since only a single observation site was available. Current efforts are concentrated on implementation of the observation operator into the MM5 3dvar system, and extensions of the observation operator to include slant-range profiler measurements. Results from these studies will be presented at the conference.

2. ARM CASE STUDY

Real-data experiments have been performed for a case over the Atmospheric Radiation Measurement (ARM) program Cloud and Radiation Testbed (CART) site in Oklahoma. The case studied here is March 19, 2000. Data assimilation runs were performed by assimilating data over a six-hour window, from 06 to 12 UTC. The initial state for the experiments was generated from a single-domain (15 km grid spacing) six-hour forecast, using the 00 UTC Eta analysis and forecast for initial and lateral boundary conditions.

A control run forecast was performed with the version of the MM5 forecast model that is part of the MM5 4dvar. The temperature and wind fields of the control run are shown in Figure 1 for level σ=0.854 (near 850 hPa). The synoptic situation is characterized by a lower level closed low associated with an upper level short-wave, which progresses east during the 6-hour assimilation time period.

A series of data assimilation runs have been performed to test the proper functioning of the 4dvar system in this configuration, and the to test and analyze the performance of the microwave profiler brightness temperature observation operator. For each experiment, a 4dvar assimilation between 06 and 12 UTC 19 March was used to arrive at an optimized set of initial conditions at 06 UTC. A forecast was then run out to 18 hours (00 UTC 20 March 2000) from these initial conditions .

* *Corresponding author address:* Thomas Nehrkorn, AER, Inc., 131 Hartwell Ave, Lexington MA 02421; email: tnehrkor@aer.com

The following table gives an overview of the data assimilation experiments. ARM sonde data was available every three hours. The raw microwave profiler data are available every 9 minutes, but in the experiments here, those data were median filtered and used at hourly intervals. Data flagged as rain-contaminated were excluded, resulting in the loss of data for the first three hours.

Table 1: Data used in the data assimilation experiments for 06-12 UTC 19 March 2000. Sonde data are the ARM sondes at the central and surrounding sites, and the microwave profiler data is from the profiler at the ARM central site.

Experiment	Sondes	Microwave Profiler	
		Retrievals	Brightness
Control			
Sonde	6, 9, 12		
MPRet		9, 10, 11, 12	
MPTb			9, 10, 11, 12

The results from these runs all show relatively small analysis increments. As is to be expected, assimilation of the sonde data resulted in the largest analysis increments. An example of the sonde run temperature increments at the end of the assimilation window is shown in Figure 2, which shows generally colder temperatures in the western half of the domain, and warmer temperatures in the eastern half. The corresponding temperature increments for the MPret and MPTb runs (not shown) are generally less than half as large as those for the sonde run, and cover a smaller area of the model domain. An example of the control and sonde and MPRet wind fields is shown Figure 3 for level σ=0.261 at hour 6. Changes in the wind fields due to assimilation of sonde data are primarily speed differences, except near the trough axis, which has a slightly sharper definition in the sonde control run. The corresponding increments in the MPRet are much smaller, with no visibly discernible differences from the control run wind.

The effects of assimilating the microwave profiler retrievals are more easily demonstrated by a comparison of measured and simulated profiler retrieval data. Figure 4 shows the microwave profiler retrievals of temperature for hours 3-18 (09 UTC 19 Mar - 00 UTC 20 Mar). Model values from the control run (interpolated to the location of the profiler) are also shown. Comparison of the control difference field shown in Figure 4 with that for the MPRet run shown in Figure 5 shows the improved fit of the model values during times within the assimilation window (09-12 UTC). During the free forecast (after 12 UTC), values at the profiler site are largely determined from grid points upstream, and differences between the two runs are much smaller.

The corresponding fits of simulated and measured brightness temperatures is summarized in Figure 6. In this case, simulated brightness temperatures for channels 9-12 are within 1-2 K of observed values during the assimilation window for all experiments, and assimilation of the brightness temperatures has a negligible impact on the fit to the observations. However, the fit to channels 1-8 is noticeably improved by assimilation of these data. As was the case in the MPRet run, however, the effects of assimilating these data are negligible at the profiler site during the free forecast.

The results from this set of assimilation experiments demonstrate the proper functioning of the 4dvar assimilation system, both for assimilation of profile data from sonde and micrwave profiler retrievals, and of profiler brightness temperatures. In this case, assimilation of 3-hourly profiles of temperature, moisture, and wind at the 5 sonde locations in the center of the domain introduced a small, but consistent change in the model fields that resulted in a slight sharpening of the short wave trough, both during the assimilation period and in the free forecast. Assimilation of hourly microwave profiler data of temperature and moisture at a single location in the model domain resulted in a better fit to the assimilated data, but had a much smaller impact at at other locations and forecast times.

3. BOULDER CASE

A second real-data case study was performed with data from a microwave profiler located in Boulder, Colorado. This case was characterized by low-level cold air advection associated with a freezing drizzle event in Boulder and Denver, where it had a significant impact on operations of the airport. This case has been the subject of studies by Herzegh et al. (2003) Ikeda and Rasmussen (2003).

For this case, a 12 km resolution grid was used for forecasts from 00 UTC 4 March 2003 (see Figure 7). The control forecast was run with initial and lateral boundary conditions derived from the 00 UTC Eta forecast. Microwave profiler temperature retrievals in Boulder, and corresponding simulated control run values, are shown in Figure 8 for this case. Boundary layer temperatures in the control are slightly colder than then the retrieved values during the first 9 hours of the forecast. The rapid cooling of the boundary layer between 08-13 UTC seen in the profiler data (as was shown in Herzegh et al., these observations are consistent with the 12 UTC Denver radiosonde sounding), are accompanied by an increase in boundary layer moisture, with maximum values at 11 UTC (see Figure 9). In the control run, these temperature changes are more gradual, and occur later. The moistening of the boundary layer is shifted almost 10 hours in time in the control run. An initial set of assimilation experiments was performed with an assimilation time window of 00 - 06 UTC, before the onset of the PBL cooling and moistening in Denver and Boulder.

The effects of assimilating retrieved profiles on forecast values at the profiler site is shown in Figure 10. Comparison with the corresponding plots for the control run shows an improved fit to the temperature and moisture (the latter more so at the initial time) during the assimilation time period, but little effect during the free forecast. Differences from the control run are larger at other grid locations, but there is no consistent improvement in the forecast evolution of the intrusion of the cold, moist boundary layer air form the Northeast.

The evolution of observed and simulated brightness temperatures at the Boulder profiler location is shown in Figure 11. The brightness temperatures for channels 1-8 clearly show the signature of cloud liquid water in the observed (at 12 UTC) and simulated (at 18 UTC) brightness temperatures. During the assimilation time window, observed and simulated brightness temperatures of these channels agree to within 1-2 K for all experiments, and assimilation of the brightness temperatures has little effect. In contrast, the brightness temperatures in channels 9-12 reflect the observed and simulated cooling of the boundary layer throughout the forecast. During the assimilation window, simulated values in the control run are too low, and the fit is improved by assimilation of the brightness temperatures, and, to a lesser extent, by assimilation of the retrieved profiles. During the free forecast, the situation is reversed, and there is no discernible difference in simulated values at the profiler site.

3. SUMMARY AND FUTURE WORK

The results demonstrate the proper implementation of the 4dvar assimilation of both retrieved profiles and brightness temperature data from the profiler. Forecast impacts are generally small in the cases studied here, since only a single observation site was available in the model domain, and errors in the control run forecasts were related to errors in the mesoscale or larger scale forcing.

Current efforts are concentrated on implementation of the observation operator into the MM5 3dvar system, and extensions of the observation operator to include slant-range profiler measurements.

4. REFERENCES

P. H. Herzegh, S. Landolt, and T. Schneider, 2003: The structure, evolution and cloud processes of a Colorado upslope storm as shown by profiling radiometer, radar and tower data. In *31st Conference on Radar Meteorology*, Seattle, WA, 2003. American Meteorological Society, Boston, MA Available from http://ams.confex.com/ams/32BC31R5C/techprogram/paper_64469.htm.

K. Ikeda and R. M. Rasmussen, 2003: Radar observations of a freezing drizzle case in Colorado. In *31st Conference on Radar Meteorology*, Seattle, WA, 2003. American Meteorological Society, Boston, MA. Available from http://ams.confex.com/ams/32BC31R5C/techprogram/paper_64788.htm.

Ware, R., R. Carpenter, J. Güldner, J. Liljegren, T. Nehrkorn, F. Solheim and F. Vandenberghe, 2003: A multichannel radiometric profiler of temperature, humidity, and cloud liquid, *Radio Science*, 38, 8079, doi:10.1029/2002RS002856.

5. ACKNOWLEDGEMENTS

This work was supported by Army Research Laboratory contract DAAD17-01-C-0045. The authors thank Francois Vandenberghe of NCAR for the software for the computation of the simulated retrieval profiles.

6. FIGURES

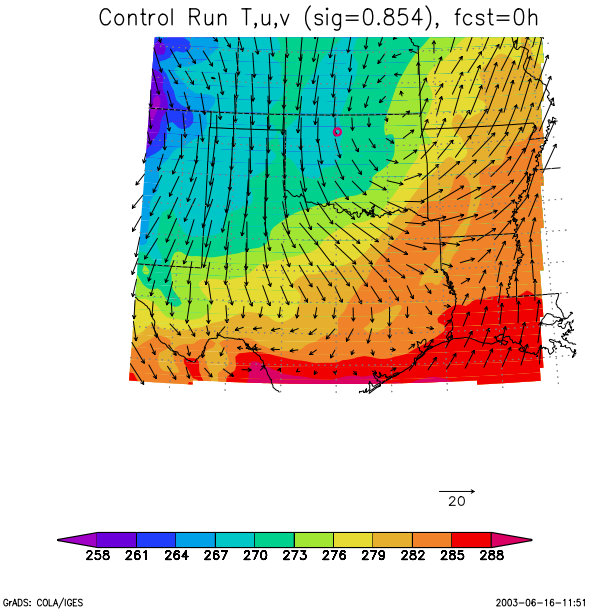

Figure 1: Control wind field (m/s) and temperature (K) at σ=0.854, at hour 0 (06 UTC, top panel) and 6 (12 UTC, bottom panel). The profiler location is indicated by the red circle.

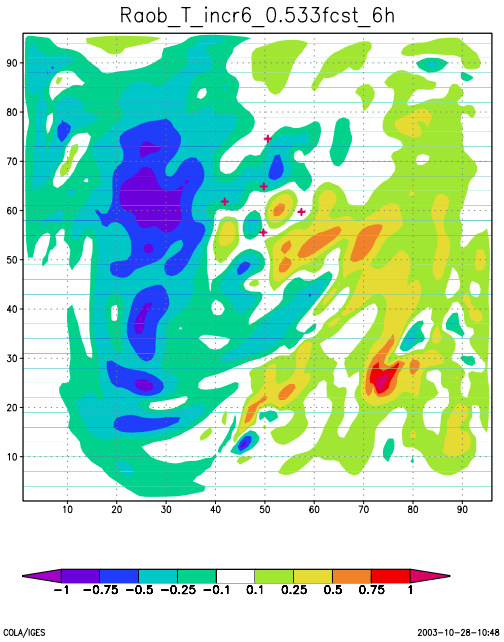

Figure 2: Sonde run temperature analysis increments (sonde-control) at hour 6 (12 UTC), at σ=0.533. The model domain corresponds to the geographic area shown in Figure 1. The axes are labeled by gridpoint index, and the sonde data locations are shown as red crosses.

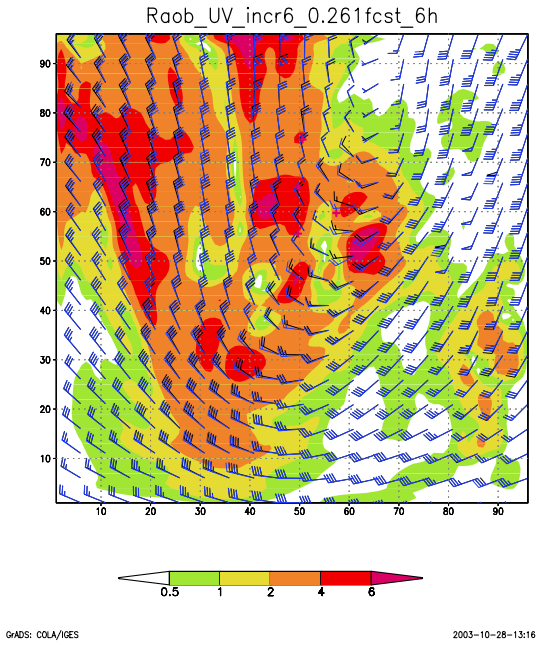

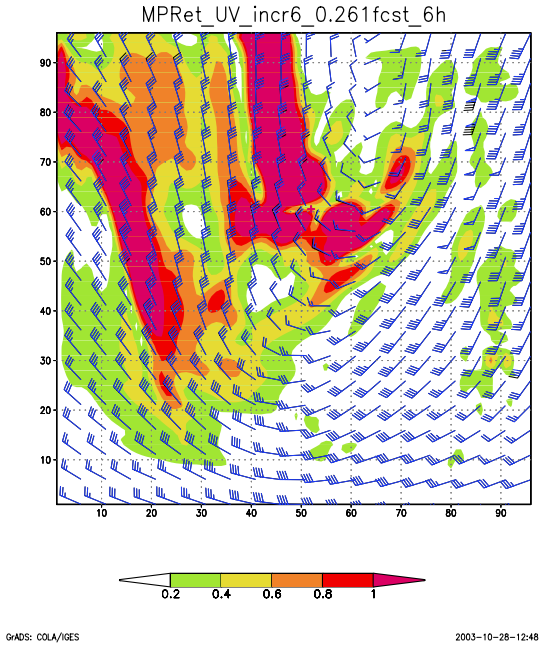

Figure 3: Wind fields at σ=0.261. The control run wind field is shown in black (a full barb corresponds to 10 m/s), and sonde run (top panel) or MPRet run (bottom panel) wind fields are overplotted in blue. The respective data locations for each run are marked by red crosses. The color shading indicates the analysis increment vector magnitude (note the change in scale between the panels).

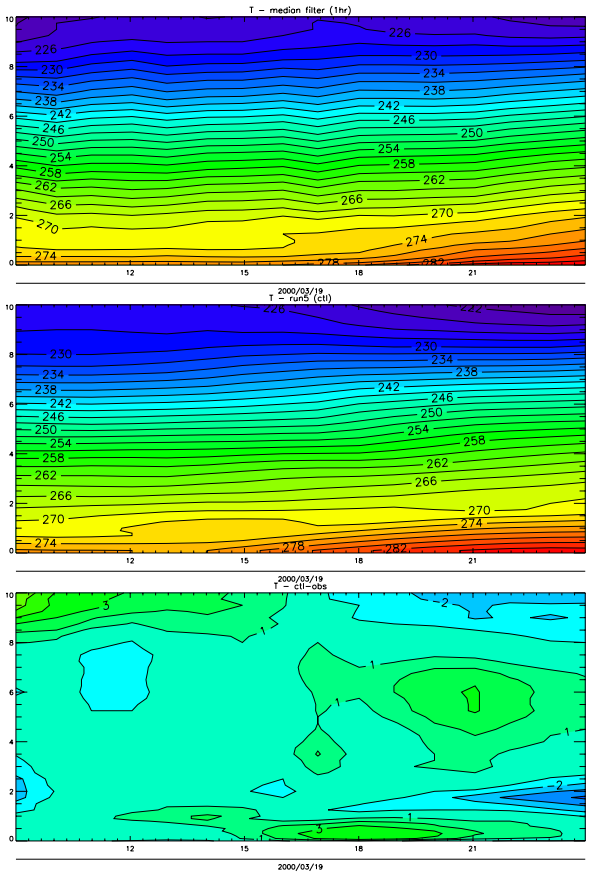

Figure 4: Time-height section of observed (top panel), simulated (center panel), and differences between simulated and observed (bottom panel) temperatures (K) at the microwave profiler location for the ARM control run.

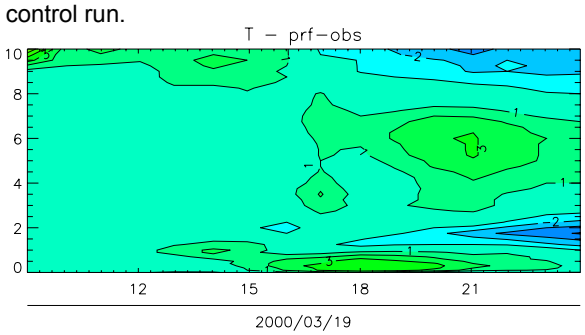

Figure 5: Differences between simulated and observed temperatures (K) at the microwave profiler location for the ARM MPRet run.

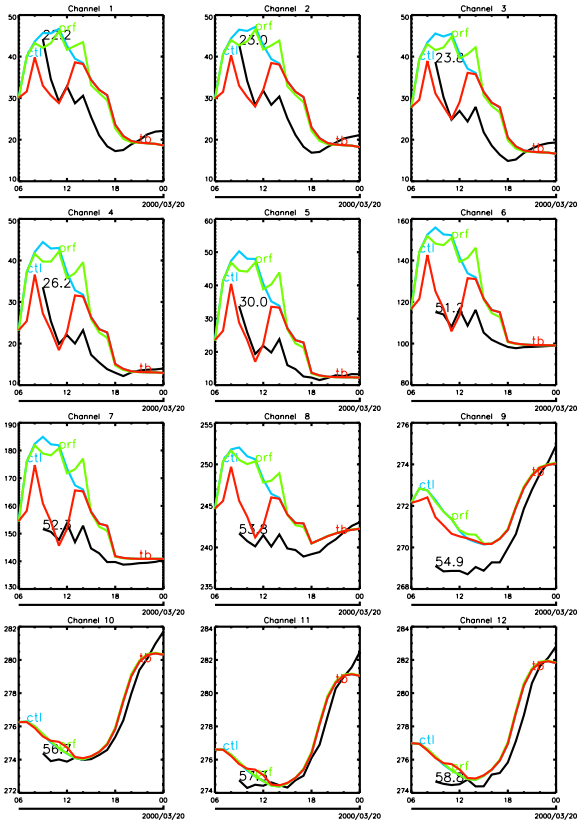

Figure 6: Observed and simulated brightness temperatures for channels 1-12, for the ARM case. Observed values are shown in black (black labels indicate the frequency in GHz), control run simulated values in blue, MPRet run values in green, and MPTb run values in red.

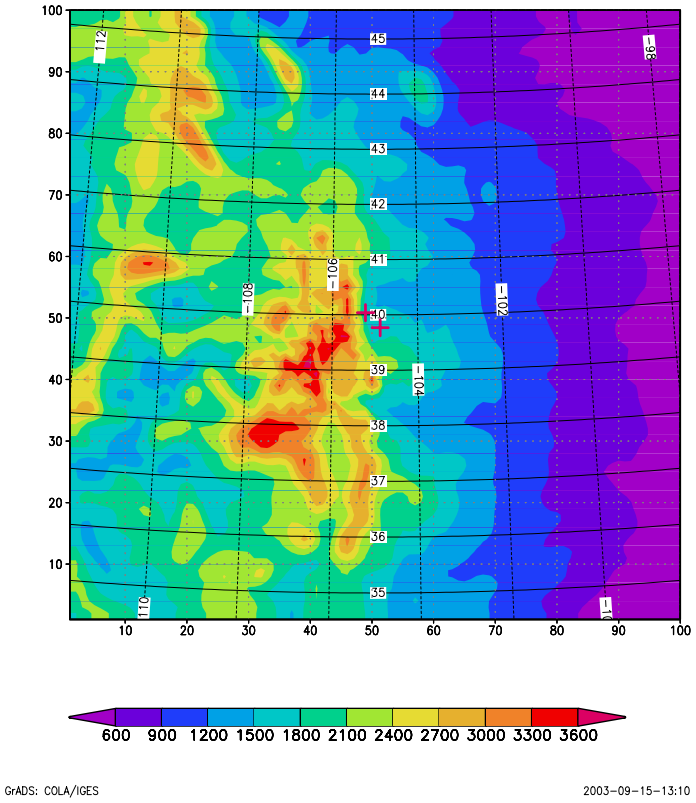

Figure 7: The model terrain (m) for the domain used for the Boulder case. The axes are label by grid point index, and lines of constant latitude and longitude are overlaid. The grid spacing is 12 km. The location of the Denver radiosonde and the Boulder microwave profiler are shown as red crosses.

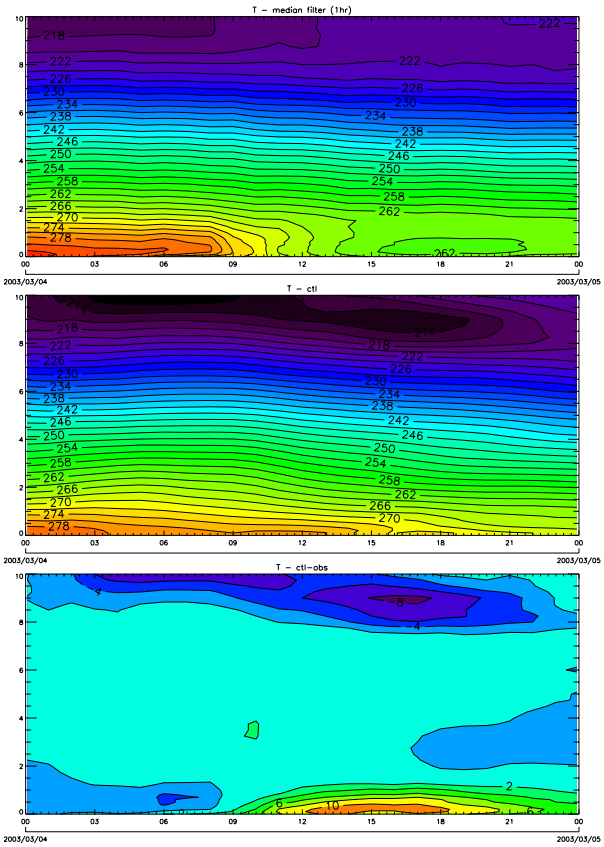

Figure 8: Observed (top panel), simulated (center panel), and differences between simulated and observed (bottom panel) temperatures (K) for the Boulder control run.

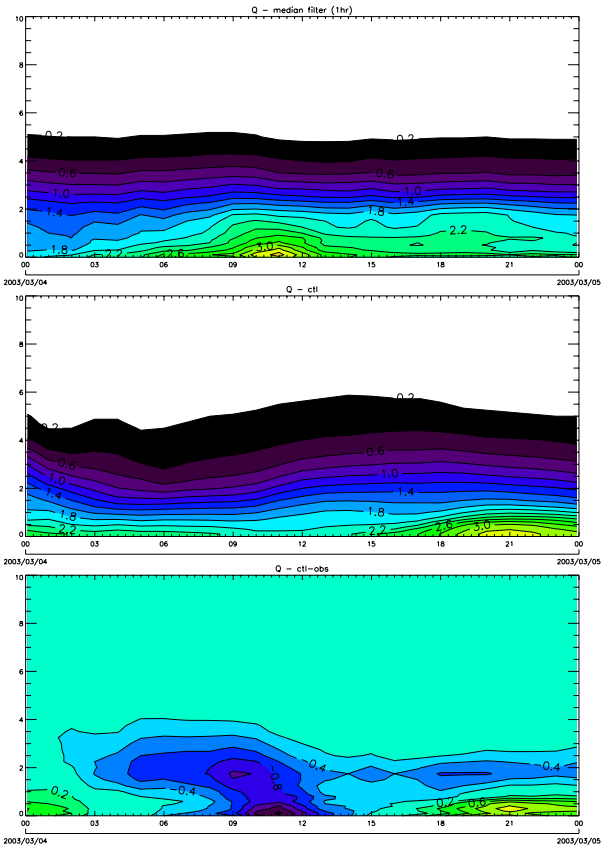

Figure 9: Observed (top panel), simulated (center panel), and differences between simulated and observed (bottom panel) water vapor density (g/m^3) for the Boulder control run.

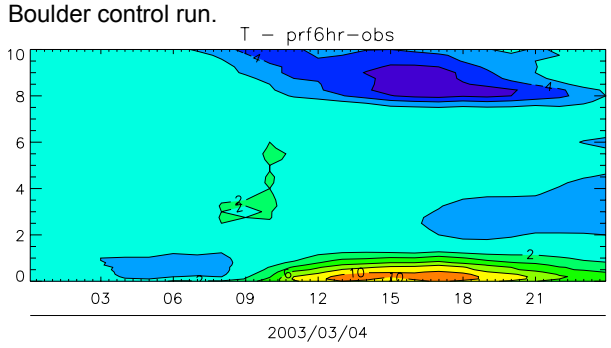

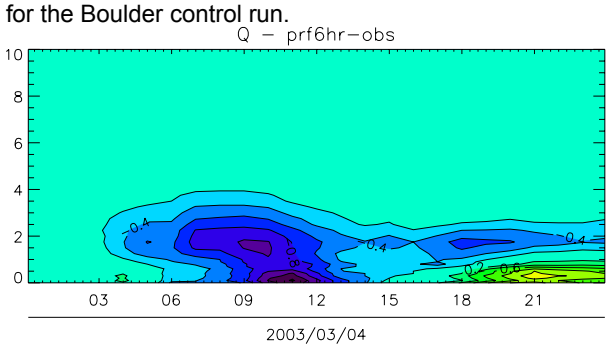

Figure 10: Differences between simulated and observed profiler temperature (left panel) and moisture (right panel) profiles in Boulder for the retrieval assimilation run.

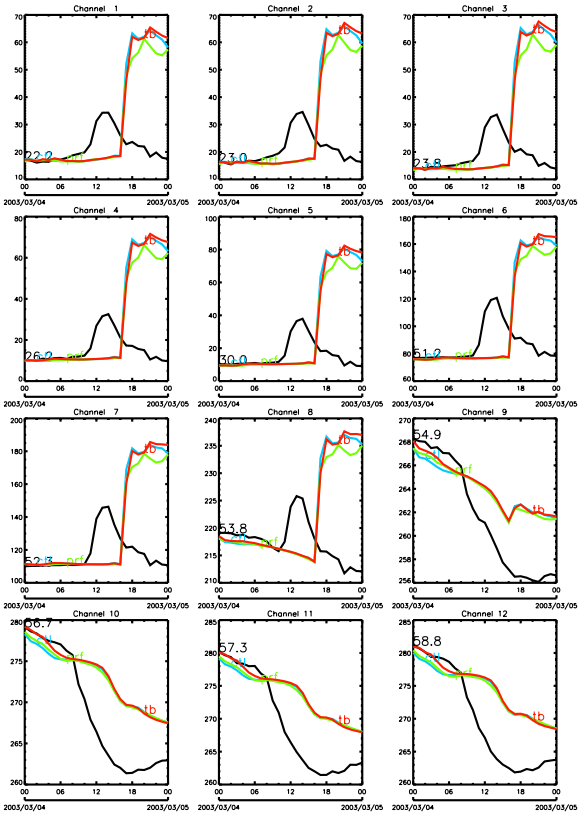

Figure 11: Observed and simulated brightness temperatures for channels 1-12, for the Boulder case. Observed values are shown in black (black labels indicate the frequency in GHz), control run simulated values in blue, MPRet run values in green, and MPTb run values in red.